

Original Article

Hepato-splenic axis: hepatic and splenic metabolic activities are linked

Georgia Keramida^{1,2}, Alexander Dunford³, Guven Kaya³, Constantinos D Anagnostopoulos⁴, Adrien Michael Peters^{2,3}

¹Royal Brompton and Harefield NHS Trust, London, UK; ²Clinical Imaging Sciences Centre, Brighton Sussex Medical School, Brighton, UK; ³Brighton and Sussex University Hospitals NHS Trust, Brighton, UK; ⁴Center for Experimental Surgery, Clinical and Translational Research, Biomedical Research Foundation Academy of Athens, Greece

Received April 25, 2018; Accepted May 22, 2018; Epub June 5, 2018; Published June 15, 2018

Abstract: The concept of a hepato-splenic axis has recently been put forward. We aimed to investigate whether hepatic and splenic metabolic activities are linked, and if splenic metabolic activity is increased in non-alcoholic fatty liver disease (NAFLD). Blood clearance rates of phosphorylated ¹⁸F-fluorodeoxyglucose were measured in the spleen and liver from dynamic PET using Gjedde-Patlak-Rutland graphical analysis and abdominal aorta for input function in 59 patients undergoing routine PET/CT. Plot gradient (Ki), which represents blood clearance, was divided by intercept (V(0)), which represents tissue FDG distribution volume, and multiplied by blood glucose to give glucose uptake rate per unit tracer distribution volume (MRglu). In addition, liver-to-spleen raw count rate ratio was plotted against time, and gradient (b) divided by intercept (A) to obtain hepatic-to-splenic blood clearance ratio independent of aortic input function. Hepatic steatosis was inferred when hepatic CT density was ≤ 40 HU. There was no difference in splenic MRglu between 8 patients with inactive lympho-proliferative disease (LPD) as identified by negative PET/CT, 25 with non-haematological malignancy and 13 with normal PET/CT. It was significantly increased in 13 with active LPD, who were therefore excluded, along with 3 more with type-2 diabetes mellitus. Splenic MRglu was higher in patients with hepatic steatosis (4.0 ± 1.6 ; n = 12) than without (2.6 ± 1.7 $\mu\text{mol}/\text{min}/100$ ml; P = 0.02) and correlated inversely with hepatic CT density (r = -0.49; P < 0.001). Hepatic and splenic Ki/V(0) correlated (r = 0.52; P < 0.01) in 22 patients in whom the correlation coefficient between b/A and hepatic-to-splenic Ki/V(0) ratio was 0.99 and in whom, therefore, input function errors in graphical analysis could be discounted. In men, splenic longitudinal diameter correlated significantly with hepatic CT density (r = -0.35; P = 0.046), hepatic MRglu (r = 0.44; P = 0.005) and splenic MRglu (r = 0.35; P = 0.046). Splenic Ki/V(0) correlated positively with blood glucose, suggesting sensitivity to insulin. We conclude that hepatic and splenic metabolic activities are linked and that a speculative mechanism, which deserves further investigation, is shared insulin sensitivity. Splenic MRglu and spleen size are increased in NAFLD.

Keywords: Glucose, FDG, PET, spleen, liver, metabolic rate

Introduction

Tarantino et al recently reviewed the extent to which hepatic and splenic functions are linked, and coined the term hepato-splenic axis [1]. It is well known that some functions, for example reticulo-endothelial function, are shared between liver and spleen but other functional links are emerging, especially in non-alcoholic fatty liver disease (NAFLD), which is associated with increased hepatic glucose uptake [2, 3] and in which splenic enlargement has been noted in the absence of cirrhosis [1, 4-7].

NAFLD, which comprises non-alcoholic steatohepatitis (NASH) and simple steatosis, is becoming increasingly important in the Western World as a result of the obesity epidemic and associated metabolic syndrome. The majority of patients with NAFLD (90%) have simple steatosis [8], which is benign. NASH, however, is not benign because it eventually progresses to hepatic fibrosis and cirrhosis [9], and is overtaking alcoholic steatohepatitis (ASH) as the leading indication for liver transplantation [10]. There is great interest in non-invasive diagnostic techniques that can distinguish between

Hepato-splenic axis

simple steatosis and NASH because currently a definitive diagnosis of NASH requires liver biopsy. Splenic enlargement is one such proposed simple test [4], but in the context of a hepato-splenic axis, indices of splenic function as well as size are also of increasing interest.

A shared role between liver and spleen has also been described in cardiovascular disease with which NAFLD is associated [11, 12], although it remains contradictory whether the spleen plays a protective role, such as by reducing circulating levels of lipids [13, 14], or a counter-protective role through macrophage-stimulation of arterial wall inflammation [15-18], with which hepatic steatosis is also associated [19].

To our knowledge, no previous studies have addressed metabolic coupling between the liver and spleen or measured splenic metabolic activity in NAFLD, in addition to spleen size. The aim of our study therefore was to use dynamic positron emission tomography (PET) and the glucose analogue, ^{18}F -fluorodeoxyglucose (FDG), to investigate the hypothesis that liver and spleen are metabolically coupled and also investigate whether splenic metabolic activity is increased in patients with NAFLD.

Material and methods

Patients

The patients were from a population of 60 undergoing routine FDG PET/CT, mostly for management of malignancy, reported elsewhere [2, 20, 21]. One with previous splenectomy was excluded, leaving 46 men (age range 28-83) and 13 women (age range 42-67). Five patients had proven diabetes mellitus. We did not include patients with known or suspected high alcohol intake.

The patients were divided into 4 groups according to their PET/CT images as follows: 1) Patients with FDG-avid (i.e. active) lympho-proliferative disease (LPD) ($n = 13$). 2) Patients with inactive LPD ($n = 8$). 3) Patients with abnormal PET/CT showing FDG-avid malignancy other than LPD ($n = 25$). 4) Patients with no history of LPD and normal PET/CT ($n = 13$).

All patients gave written informed consent for inclusion in the study, which was approved by a local institutional review board.

Imaging

Patients fasted for 6 h. Blood glucose was measured immediately before FDG injection using a glucometer (ACCU-CHEK Performa; Inform II strips; Roche, Burgess Hill, Sussex, UK). Dynamic PET was performed in single bed position over the upper abdomen and chest following i.v. injection of 400 MBq ($\pm 10\%$) FDG, acquiring 30×1 min frames, using a Siemens Biograph 64-slice 16 Truepoint PET/CT scanner (Erlangen, Germany), as previously described [2, 20, 21]. Routine whole body PET/CT was then performed at 60 min post-injection, as previously described [2, 20, 21].

Dynamic image analysis

The blood clearance into the liver of FDG that undergoes phosphorylation (ml/min per ml of liver tissue) is known as uptake constant (K_i) and is related to the tissue concentration of phosphorylated FDG (FDG6P) and blood concentration ($C(t)$) of un-phosphorylated FDG as follows.

$$\text{FDG6P} = K_i \cdot C(t) \cdot dt \quad (1)$$

The concentration of tracer in tissue detected by the PET scanner, however, is equal to the sum of the concentrations of FDG and FDG6P. Therefore, adding FDG to both sides of equation 1 and dividing through by $C(t)$ gives the classical Gjedde-Patlak-Rutland equation.

$$\frac{\text{FDG}(t) + \text{FDG6P}(t)}{C(t)} = K_i \cdot T + \frac{\text{FDG}(t)}{C(t)} \quad (2)$$

where T is the ratio of the integrated blood concentration divided by instantaneous blood concentration and called normalized time. K_i (ml/min/ml) is the gradient of the plot of tissue-to-blood concentration ratio against T . FDG exchanges between tissue and blood via K_1 (blood clearance of FDG into tissue) and k_2 transport constant of FDG from tissue to blood. When mixing of FDG between blood and tissue is complete $\text{FDG}(t)/C(t)$ is constant, referred to as the distribution volume ($V(0)$; ml/ml) and is given by the intercept of the plot, at which time, theoretically, no tissue FDG6P has yet been generated.

The PET images need to be corrected for photon attenuation in order to obtain K_i and $V(0)$.

Hepato-splenic axis

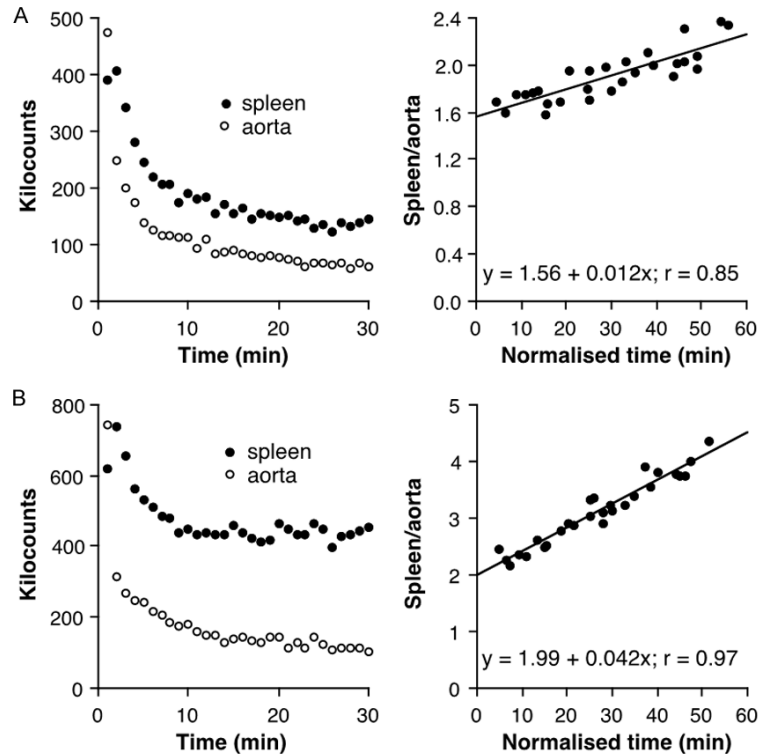


Figure 1. Gjedde-Patlak-Rutland plots in (A) a patient without lympho-proliferative disease and (B) a patient with lympho-proliferative disease. Vertical co-ordinates are raw counts in thousands and horizontal co-ordinates are normalized time (min). Equations from linear regression analysis, shown in right panels, give $K_i/V(0)$ values of 0.77 ml/min/100 ml (upper panel) and 2.11 ml/min/100 ml (lower panel). Note that the first 2 points in the right panels have been excluded, after which the plots appear linear.

separately in absolute units. However, we did not perform attenuation correction but instead recorded raw counts from liver/spleen and blood, and divided the gradient by the intercept, effectively normalizing K_i to $V(0)$, as previously described [2, 20, 21]. This approach is therefore valid, as proved elsewhere, because the proportionality constants that respectively relate gradient to K_i and intercept to $V(0)$ are identical and cancel out [2]. $K_i/V(0)$ was then multiplied by the blood glucose concentration to give $MRglu$ in units of $\mu\text{mol}/\text{min}/100\text{ ml}$. We assumed a lumped constant of unity for both tissues [22].

Liver and spleen raw counts were each summed from circular regions of interest (ROIs) of 3 cm and 2.5 cm diameter, respectively, on about 20 contiguous transaxial images. Raw counts in blood (arterial input function) were summed in ROIs of 1.6 cm diameter, carefully placed within the lumen of the abdominal aorta and avoiding the wall, from about 20 transaxial

images. Other workers have validated the use of the abdominal aorta for input function in Gjedde-Patlak-Rutland graphical analysis [23, 24]. We did not use the cardiac ventricular cavities for input function because the heart was not always fully included in the field-of-view during the dynamic study.

Mixing of FDG between blood and the liver and spleen distribution volumes was assumed to be complete within 3 min of FDG injection, so the first 2 frame values were not included in the Gjedde-Patlak-Rutland plot for either tissue but nevertheless included in the calculation of normalized time. As in studies of others on the liver [25-28], inspection of both plots revealed that they were essentially linear between 3 and 30 min scan time, consistent with this assumption (**Figure 1**), and with the assumption of negligible dephosphorylation of FDG6P over this period of time.

Because it can be assumed that FDG does not enter the fat droplets in hepatocytes, the normalization of K_i to $V(0)$ has the attraction of avoiding the physical 'dilutional' effect of hepatic fat on K_i and effectively gives FDG clearance as ml/min per ml of lean liver.

As a 'gold standard' measure of relative hepatic and splenic K_i values, independent of aortic input function in graphical analysis, we also plotted the ratio of raw liver-to-spleen counts as a function of scan time and divided the gradient (b) by the intercept (A) (**Figure 2**). If there were no input function errors in Gjedde-Patlak-Rutland analysis, especially partial volume errors from the abdominal aorta, b/A should show a very close correlation with the ratio of hepatic-to-splenic $K_i/V(0)$. Moreover, this relationship will have an intercept of unity because when hepatic and splenic $K_i/V(0)$ are identical, b/A will be zero. Input errors will decrease the hepatic-to-splenic $K_i/V(0)$ ratio when splenic $K_i/V(0)$ exceeds hepatic $K_i/V(0)$ and increase

Hepato-splenic axis

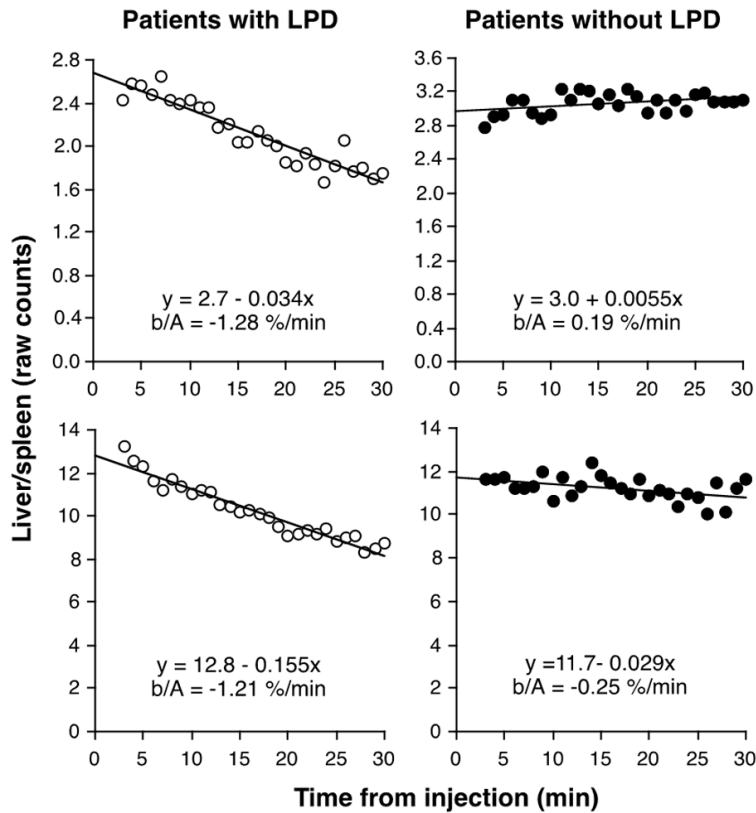


Figure 2. Hepatic-to-splenic raw count rate ratios as functions of scan time. As for the Gjedde-Patlak-Rutland plots, the first two points were excluded. Left panels: patients with lympho-proliferative disease (LPD); right panels: patients without lympho-proliferative disease. The value of gradient (b) divided by intercept (A) is shown for each patient.

the ratio when hepatic $K_i/V(0)$ exceeds splenic $K_i/V(0)$, respectively displacing points downwards or upwards in the relationship between b/A and $K_i/V(0)$ ratio.

Whole body image analysis

Standardized uptake value (SUV) is widely used as the conventional parameter for semi-quantification of tissue FDG accumulation. SUV was measured from the 60 min whole body PET/CT scan from ROIs of 2 cm and 3 cm diameter respectively placed over the spleen and right lobe of the liver. SUV, both as pixel maximum (SUV_{max}) and pixel average (SUV_{mean}), was recorded from the following formula.

$$SUV = \text{MBq/ml} \times (\text{body weight/administered activity}) \quad (3)$$

Mean splenic and hepatic CT densities were obtained from the unenhanced CT scan us-

ing the same ROIs from which SUVs were obtained. With respect to the liver, CT density ≤ 40 HU was considered to indicate hepatic steatosis [29].

The size of the spleen was measured from the 60 min PET/CT scan as the longitudinal diameter in the coronal plane, as in previous studies on the relation between NAFLD and spleen size [5-7].

Statistics

Values are expressed as mean \pm standard deviation and differences assessed using Student paired or unpaired *t*-test, as appropriate. Group differences were assessed using ANOVA. Correlation analysis was performed using Pearson regression analysis. Results were considered statistically significant when $P < 0.05$.

Results

MRglu in LPD

Splenic $K_i/V(0)$, MRglu and SUV, but not their hepatic equivalents, were all significantly higher in patients with active LPD (**Table 1**) compared with the other 3 groups. This was reflected by b/A , which was significantly lower (i.e. strongly negative) in active LPD patients (**Figure 2**; **Table 1**). Patients with active LPD (group 1) were therefore excluded from further analysis. There was no significant difference in hepatic or splenic $K_i/V(0)$, MRglu, b/A and SUV between groups 2-4 so they were combined into one group for further analysis. Three patients from this combined group with type-2 diabetes mellitus were also excluded, leaving a total of 43 patients for further analysis of whom 33 were men.

Patients with recent chemotherapy

Neither hepatic nor splenic MRglu was significantly different in patients who had received chemotherapy within 6 months of their PET/CT ($n = 10$) compared to those who had not

Hepato-splenic axis

Table 1. Hepatic and splenic Ki/V(0), glucose uptake rates (MRglu), SUV_{max} and b/A in groups 1 to 4 (n = 59)

Group (n)	Ki/V(0)		MRglu		SUV _{max}		b/A
	ml/min/100 ml		μmol/min/100 ml				%/min
	Liver	Spleen	Liver	Spleen	Liver	Spleen	
1. (13)	0.37 (0.20)	1.01 (0.59)*	2.4 (1.6)	6.4 (4.2)*	3.3 (0.7)	2.7 (0.8) [†]	-0.52 (0.55)*
2. (8)	0.32 (0.23)	0.49 (0.23)	1.6 (1.3)	2.7 (1.3)	3.4 (1.0)	2.3 (0.6)	-0.15 (0.15)
3. (25)	0.42 (0.21)	0.52 (0.26)	2.5 (1.3)	3.1 (1.8)	3.2 (0.7)	2.3 (0.5)	-0.12 (0.23)
4. (13)	0.33 (0.20)	0.50 (0.30)	2.0 (1.4)	3.0 (2.0)	3.1 (0.6)	2.3 (0.5)	-0.22 (0.34)

Group 1 significantly higher compared with groups 2-4 combined (*P<0.001; [†]P = 0.03). Group 1: active LPD (abnormal PET/CT); group 2: inactive LPD (normal PET/CT); group 3: abnormal PET/CT (not LPD); group 4: normal PET/CT (no history of LPD).

Table 2. Hepatic and splenic metabolic activities (MRglu; μmol/min/100 ml), blood glucose concentration (mmol/l), hepatic and splenic CT densities (CTD; HU) and gender (male/female) in relation to recent chemotherapy (n = 43)

	MRglu		Glucose	CTD		Gender
	Liver	Spleen		Liver	Spleen	M/F
Recent chemotherapy (within 6 months of PET/CT)						
Yes (n = 10)	2.1 (1.4)	2.3 (0.9)	5.7 (0.6)	45 (11)	41 (6)	8/2
No (n = 33)	2.1 (1.2)	3.1 (1.9)	5.8 (0.7)	47 (9)	38 (7)	25/8
<i>p</i>	>0.2	= 0.2	>0.2	>0.2	>0.2	>0.2

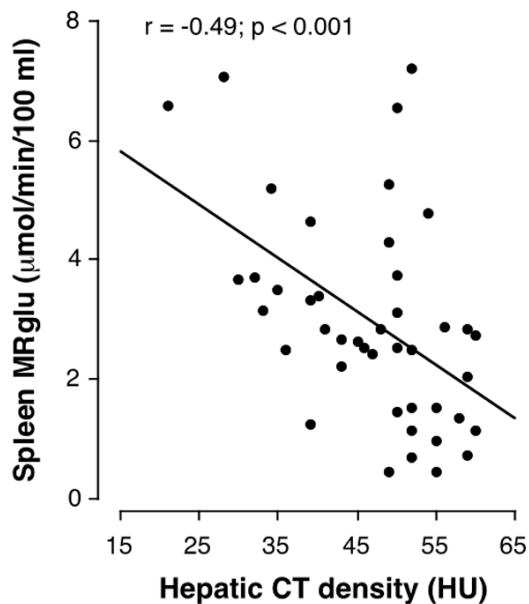


Figure 3. Splenic MRglu correlates inversely with hepatic CT density. Linear regression line shown.

received recent chemotherapy (n = 33; **Table 2**). Chemotherapy history was therefore disregarded in the ensuing analysis.

CT density

Twelve patients had hepatic steatosis, as defined above. Overall, hepatic CT density was

higher than splenic CT density with respective mean values of 47±10 HU and 39±7 HU (P<0.001) but they did not correlate significantly (r = 0.27; P = 0.08). As shown previously for the entire population of 60 patients [2], hepatic CT density correlated inversely with hepatic MRglu (r = -0.53; P<0.001) but there was no correlation between splenic CT density and splenic MRglu (r = 0.13; P = 0.4).

Splenic metabolic activity in hepatic steatosis

Splenic MRglu was higher in patients with hepatic steatosis (4.0±1.6; n = 12) than those without (2.6±1.7 μmol/min/100 ml; n = 31; P = 0.02). Corresponding values for hepatic MRglu were 3.0±1.0 and 1.7±1.2 μmol/min/100 ml (P = 0.001). Splenic MRglu correlated inversely with hepatic CT density (r = -0.49; P<0.001; **Figure 3**).

Spleen size

Spleen longitudinal diameter was greater in men (109±15 mm) than women (98±14 mm; P = 0.048) so the genders were separated for assessment of correlations of metabolic variables with spleen size. In men, spleen longitudinal diameter was significantly greater in patients with hepatic steatosis (118±13 mm; n = 10) compared with those without (105±15 mm;

Hepato-splenic axis

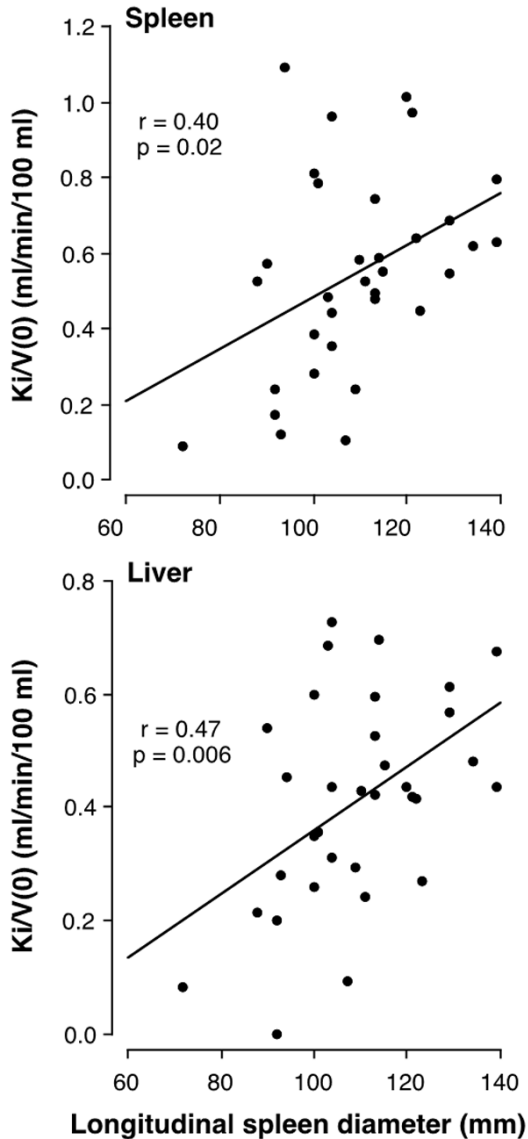


Figure 4. Spleen longitudinal diameter correlates with both splenic ($r = 0.40$; $P = 0.02$; upper panel) and hepatic ($r = 0.47$; $P = 0.006$; lower panel) $Ki/V(0)$.

$n = 23$; $P = 0.02$) and correlated with hepatic CT density ($r = -0.35$; $P = 0.046$). In men, spleen longitudinal diameter correlated significantly with hepatic MRglu ($r = 0.44$; $P = 0.005$), with splenic MRglu ($r = 0.35$; $P = 0.046$) and even more strongly with corresponding values of $Ki/V(0)$ (**Figure 4**). Spleen longitudinal diameter did not correlate with splenic CT density ($r = 0.17$; $P = 0.17$). Similar relationships were seen in women but none were significant as a result of small size of the group (and only two had hepatic steatosis).

Hepatic and splenic metabolic activities are linked

Hepatic SUV_{max} (3.2 ± 0.6) and SUV_{mean} (2.4 ± 0.4) were higher than splenic SUV_{max} (2.3 ± 0.5 ; $P < 0.0001$) and SUV_{mean} (1.9 ± 0.3 ; $P < 0.0001$). However, hepatic-to-splenic SUV ratio did not correlate with either b/A or hepatic-to-splenic $Ki/V(0)$ ratio, suggesting that SUV is a poor marker of metabolism in liver and/or spleen. SUV was therefore subjected to no further analysis.

Unlike SUV, $Ki/V(0)$ was higher in spleen (0.50 ± 0.27 ml/min/100 ml) than liver (0.36 ± 0.21 ml/min/100 ml; $P < 0.001$) with a mean ratio of 1.6 ± 1.2 . This is consistent with our previous finding that $V(0)$ is 1.6-fold higher in liver [21], indicating that hepatic and splenic glucose uptake rates per ml of *total* tissue volume are almost identical.

Hepatic $Ki/V(0)$ correlated strongly with splenic $Ki/V(0)$ ($r = 0.67$; $P < 0.001$; **Figure 5**). However, this correlation may have been artifactually strengthened by the existence of errors in the aortic input function, especially partial volume errors, impacting on both hepatic and splenic $Ki/V(0)$. We therefore used b/A, which is independent of input function in graphical analysis, as a form of quality control. The relationship between b/A and liver/spleen $Ki/V(0)$ ratio was non-linear (**Figure 5**). If there were no input function errors, b/A should correlate very closely with $Ki/V(0)$ ratio. However, 9 conspicuous outliers in a second order polynomial fit could be identified in this relationship, raising the likelihood that the graphical data in these outliers was contaminated by partial volume errors in the aortic input function. Nevertheless, when these 9 points were excluded, the correlation between hepatic and splenic $Ki/V(0)$ was still strong ($r = 0.60$; $P < 0.001$). The difference between each of the 34 points remaining after exclusion of the 9 outliers and the corresponding value given by the revised polynomial function was expressed as a percentage of the latter (% deviation). We excluded a further 12 patients with % deviation exceeding 10% to leave a population of 22 patients in which the correlation coefficient of the polynomial relationship between b/A and liver/spleen $Ki/V(0)$ ratio was 0.99 and in whom, therefore, it could be reasonably assumed that any relationship

Hepato-splenic axis

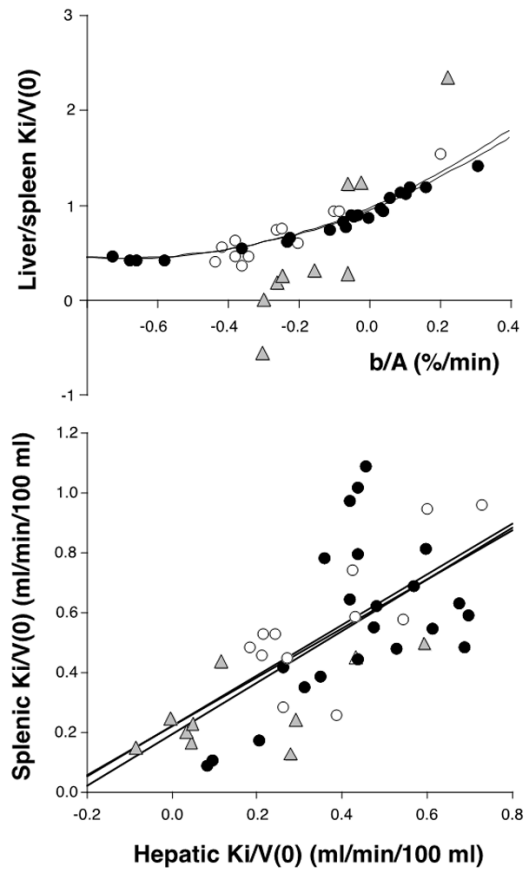


Figure 5. Upper panel: Relationship between b/A derived from raw hepatic and splenic counts (%/min) and hepatic/splenic $Ki/V(0)$ ratio ($n = 43$). Triangles ($n = 9$) were judged visually to be conspicuous outliers and excluded. The 2nd order polynomial regression line obtained after their exclusion was $y = 0.96 + 1.58x + 1.16x^2$ ($n = 34$; $r = 0.96$). Open circles display $>10\%$ deviation and closed circles $<10\%$ deviation from this regression line. The regression equation based only on closed circles ($n = 22$) is $y = 0.93 + 1.47x + 1.08x^2$ ($r = 0.99$). The two polynomial regression lines are almost indistinguishable. Lower panel: Relationships between splenic and hepatic $Ki/V(0)$ before ($n = 43$) and after exclusion firstly of 9 conspicuous outliers (triangles) and then secondly of a further 12 points (open circles) showing $>10\%$ deviation, as described above under upper panel. The 3 regression lines are almost indistinguishable and respectively given by $y = 0.20 + 0.85x$ ($r = 0.67$; $P < 0.001$; $n = 43$), $0.22 + 0.84x$ ($r = 0.58$; $P < 0.001$; $n = 34$) and $0.22 + 0.82x$ ($r = 0.52$; $P < 0.01$; $n = 22$). It can reasonably be assumed that in the final population of 22 patients (closed circles), there were no errors in the aortic input function and therefore no artifactual accentuation of the correlation between hepatic and splenic $Ki/V(0)$ values.

between hepatic $Ki/V(0)$ and splenic $Ki/V(0)$ was not the artefactual result of errors in the aortic input function used in graphical analysis.

The correlation coefficient of the relationship between hepatic $Ki/V(0)$ and splenic $Ki/V(0)$ after this second round of exclusions was 0.52 ($n = 22$; $P = 0.01$). Critically, the 3 regression equations obtained before and after these two exclusion exercises were almost identical (**Figure 5**). The correlations remained significant when patients with NAFLD were excluded.

Relationships with blood glucose

Not unexpectedly as the liver is sensitive to insulin, hepatic $Ki/V(0)$ did not show an inverse correlation with blood glucose, such as insulin-insensitive tissues like the brain would be expected to, but instead an insignificant one ($r = 0.18$; $P = 0.25$). Hepatic MRglu showed a positive correlation with blood glucose ($r = 0.36$), but, as blood glucose is present in both co-ordinates, this correlation is open to bias. Surprisingly, however, splenic $Ki/V(0)$ correlated positively and significantly with blood glucose ($r = 0.36$; $P = 0.02$; **Figure 6**), raising the possibility that the spleen, like the liver, is sensitive to insulin.

Discussion

As in previous studies [4-7], we found spleen longitudinal diameter to have a significant relationship with hepatic steatosis. However, to our knowledge, the current study is the first to measure splenic metabolic function in NAFLD and to show that the so-called hepato-splenic axis extends beyond a simple morphological relationship to one in which the metabolic activities of the two tissues may be linked, as suggested here by a significant correlation between hepatic $Ki/V(0)$ and splenic $Ki/V(0)$, increased splenic MRglu in patients with NAFLD and significant relationships between spleen longitudinal diameter and hepatic and splenic metabolic activities.

If spleen is metabolically linked to liver, then it becomes a 'new player' [1], especially in cardiovascular disease with which NAFLD is associated [11, 12] and also expands the role of the spleen in the so-called cardio-splenic axis, which describes the increased splenic metabolic activity associated with recent myocardial infarction and cardiovascular inflammation [15-18].

Assuming that negligible FDG enters hepatic fat droplets, $V(0)$ represents lean hepatic tis-

Hepato-splenic axis

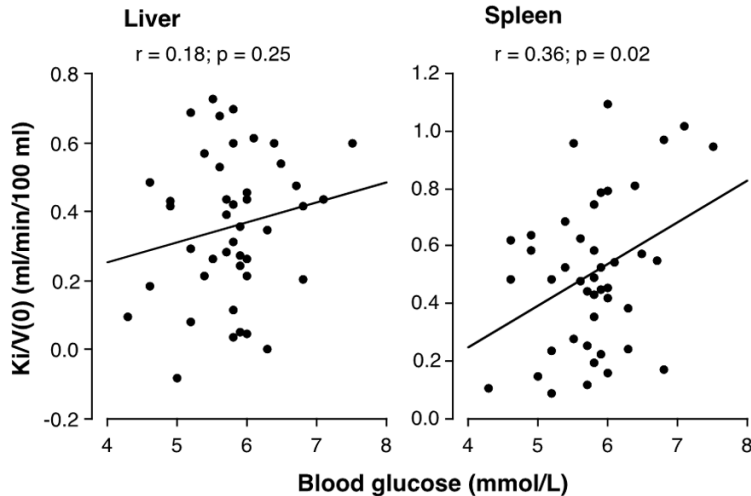


Figure 6. Neither splenic nor hepatic $K_i/V(0)$ correlates inversely with blood glucose, consistent with an increase in their MR_{glu} in response to hyperglycemia. Indeed, splenic $K_i/V(0)$ (upper panel), but not hepatic $K_i/V(0)$ (lower panel), correlates positively and significantly with blood glucose.

sue volume. Normalizing K_i to $V(0)$ therefore avoids the influence of 'dilution' of the FDG signal by hepatic fat [30]. The liver may, not uncommonly nowadays, contain as much as 30% fat, which would result, other things being equal, in K_i in hepatic steatosis being about 25% less than in lean liver. This physical influence of hepatic fat on K_i has not been considered in previous studies in which hepatic glucose uptake was measured using dynamic FDG PET [31-34], even though some patients were morbidly obese [34]. Nor has the effect of splenic fat on splenic K_i been addressed. Considering, however, that splenic CT density is generally less than hepatic CT density, splenic fat may carry the same significance. Higher fat content of the spleen would partially explain why FDG distribution volume is lower in the spleen (~ 0.55 ml/ml [21]) compared with healthy liver (~ 0.85 [25, 31, 32]). $V(0)$ in fatty liver has not been reported but would be expected to be reduced. An analogous situation is encountered in the lungs for which previous workers have normalised the Gjedde-Patlak-Rutland plot gradient to intercept in order to account for variations in lung air volume [35, 36].

The first two points of the Patlak-Rutland plots were excluded from linear regression analysis to allow for mixing of FDG throughout its tissue distribution volume. Exclusion of more

points, as generally performed in equivalent analyses of brain and myocardial FDG studies, was not considered necessary as the mixing time of FDG in liver and spleen appears to be rapid, and more rapid than in brain or myocardium because the liver and spleen are furnished with fenestrated endothelium, in contrast to the continuous and less permeable endothelia of brain and myocardium. For example, K_1 and k_2 are both about 10-fold higher in the liver compared with brain [31, 32, 37]. Mixing within 2-3 min is compatible with published values of K_1 and k_2 for the liver (0.62-1.07 and 0.67-1.9 min^{-1} , respectively [25, 31, 32]). The sum of these

two rate constants approximates to the rate constant of mixing [38], about 1.29-2.97 min^{-1} , which in turn gives a time to 95% mixing of 1.0-2.3 min.

Limitations of this study include use of a heterogeneous patient population with cancer, which inevitably results in poor patient characterization. Correlations involving SUVs are prone to artifact for several reasons, including their dependence on statistical noise [39], blood glucose level [40] and whole body metric used to calculate them [41]. It is invalid to correlate one tissue SUV against another because both contain patient weight (or other whole body metric, such as lean body mass) and administered activity in their calculations, even though several previous studies have reported such correlations [16, 17]. Moreover, liver/spleen SUV ratio showed no correlation with b/A or with the hepatic-to-splenic $K_i/V(0)$ ratio. Even at 60 min post-injection, the majority of FDG in spleen ($\sim 65\%$) and liver ($\sim 75\%$) remains un-phosphorylated [21, 42], so SUV is a poor marker of metabolism in liver and spleen.

Insufficient patients were recruited in this study to distinguish between simple hepatic steatosis and NASH. Thus, the patient population included a total of only 12 patients with NAFLD so, assuming that 10% of NAFLD patients have NASH [8], our population would only have included one or two patients with NASH.

An important limitation is that for graphical analysis we used the same arterial input function for both tissues, which may have generated a spurious correlation between their metabolic activities. In particular, partial volume errors from the abdominal aorta may have deviated the gradients of the hepatic and splenic Gjedde-Patlak-Rutland plots in the same direction. In an attempt to evaluate the potential impact of this, we plotted the raw liver-to-spleen activity ratio as a function of time and used it as a 'gold standard' to check the ratio of liver-to-spleen $K_i/V(0)$ values. Partial volume errors in input function would tend to increase the aortic signal and thereby reduce both hepatic and splenic $K_i/V(0)$. This would have an effect on their ratio, either reducing it when $K_i/V(0)$ is lower for the liver than spleen, or increasing it *vice versa*. However, outliers in this relationship would not necessarily be the result of error but alternatively the result of 'true' low values of $K_i/V(0)$ for liver or spleen which would render the $K_i/V(0)$ ratio more susceptible to noise in general. For this reason we did not exclude outliers from our other analyses, only the correlation between liver and spleen $K_i/V(0)$ values. Having rigorously excluded outliers, including even borderline outliers, to generate a population of patients in which the correlation between b/A and the $K_i/V(0)$ ratio was very high ($r = 0.99$), we still obtained a highly significant correlation between hepatic and splenic $K_i/V(0)$ values, supporting the contention that liver and spleen are metabolically linked. This latter correlation remained significant when patients with NAFLD were excluded, suggesting that linking is a general phenomenon.

A speculative factor that may contribute to such linking is insulin sensitivity. In tissues that are insensitive to insulin, such as the brain [43, 44], FDG clearance varies inversely with blood glucose as a result of competition with glucose for tissue accumulation. In insulin-sensitive tissue, in contrast, the insulin-stimulated increase in FDG phosphorylation that follows an increase in blood glucose *may* override competition with glucose and increase FDG clearance [31, 32, 44, 45]. Although hepatic $K_i/V(0)$ showed no correlation with blood glucose, splenic $K_i/V(0)$ correlated with it significantly, raising the possibility that the spleen, like the liver, is sensitive to insulin.

In conclusion, we present evidence to suggest that hepatic and splenic metabolic rates are linked and that splenic glucose uptake is increased in NAFLD. The biological mechanisms, pathophysiological consequences and clinical relevance of these findings are topics for further investigation.

Acknowledgements

The authors are grateful to Dr Stephan Nekolla for constructive criticism. This research did not receive any specific grant from any funding agency in the public, commercial or not-for-profit sector.

Disclosure of conflict of interest

None.

Abbreviations

NAFLD, non-alcoholic fatty liver disease; NASH, non-alcoholic steatohepatitis; FDG, ^{18}F -fluorodeoxyglucose; PET/CT, positron emission tomography/computed tomography; LPD, lymphoproliferative disease; SUV, standardized uptake value.

Address correspondence to: Adrien Michael Peters, Department of Nuclear Medicine, Royal Sussex County Hospital, Brighton BN2 5BE, UK. Tel: 01273 523360; E-mail: a.m.peters@bsms.ac.uk

References

- [1] Tarantino G, Scalera A and Finelli C. Liver-spleen axis: intersection between immunity, infections and metabolism. *World J Gastroenterol* 2013; 19: 3534-3542.
- [2] Keramida G, Hunter J and Peters AM. Hepatic glucose utilisation in hepatic steatosis and obesity. *Biosci Rep* 2016; [Epub ahead of print].
- [3] Bural GG, Torigian DA, Burke A, Houseni M, Alkhaldeh K, Cucchiara A, Basu S and Alavi A. Quantitative assessment of the hepatic metabolic volume product in patients with diffuse hepatic steatosis and normal controls through use of FDG-PET and MR imaging: a novel concept. *Mol Imaging Biol* 2010; 12: 233-239.
- [4] Tsushima Y and Endo K. Spleen enlargement in patients with nonalcoholic fatty liver: correlation between degree of fatty infiltration in liver and size of spleen. *Dig Dis Sci* 2000; 45: 196-200.
- [5] Tarantino G, Conca P, Pisanisi F, Ariello M, Mastrolia M, Arena A, Tarantino M, Scopacasa

Hepato-splenic axis

- F and Vecchione R. Could inflammatory markers help diagnose nonalcoholic steatohepatitis? *Eur J Gastroenterol Hepatol* 2009; 21: 504-511.
- [6] Tarantino G, Colicchio P, Conca P, Finelli C, Di Minno MN, Tarantino M, Capone D and Pasanisi F. Young adult obese subjects with and without insulin resistance: what is the role of chronic inflammation and how to weigh it non-invasively? *J Inflamm (Lond)* 2009; 6: 6.
- [7] Savastano S, Di Somma C, Pizza G, De Rosa A, Nedi V, Rossi A, Orio F, Lombardi G, Colao A and Tarantino G. Liver-spleen axis, insulin-like growth factor-(IGF)-I axis and fat mass in overweight/obese females. *J Transl Med* 2011; 9: 136.
- [8] Bellentani S, Scaglioni F, Marino M and Bedogni G. Epidemiology of non-alcoholic fatty liver disease. *Dig Dis* 2010; 28: 155-161.
- [9] Vernon G, Baranova A and Younossi ZM. Systematic review: the epidemiology and natural history of non-alcoholic fatty liver disease and non-alcoholic steatohepatitis in adults. *Aliment Pharmacol Ther* 2011; 34: 274-285.
- [10] Agopian VG, Kaldas FM, Hong JC, Whittaker M, Holt C, Rana A, Zarrinpar A, Petrowsky H, Farmer D, Yersiz H, Xia V, Hiatt JR and Busuttil RW. Liver transplantation for nonalcoholic steatohepatitis: the new epidemic. *Ann Surg* 2012; 256: 624-633.
- [11] Hamaguchi M, Kojima T, Takeda N, Nagata C, Takeda J, Sarui H, Kawahito Y, Yoshida N, Suetsugu A, Kato T, Okuda J, Ida K and Yoshikawa T. Nonalcoholic fatty liver disease is a novel predictor of cardiovascular disease. *World J Gastroenterol* 2007; 13: 1579-1584.
- [12] Anstee QM, Targher G and Day CP. Progression of NAFLD to diabetes mellitus, cardio-vascular disease or cirrhosis. *Nat Rev Gastroenterol Hepatol* 2013; 10: 330-344.
- [13] Akan AA, Sengül N, Simşek S and Demirer S. The effects of splenectomy and splenic auto-transplantation on plasma lipid levels. *J Invest Surg* 2008; 21: 369-372.
- [14] Rezende AB, Neto NN, Fernandes LR, Ribeiro AC, Alvarez-Leite JI and Teixeira HC. Splenectomy increases atherosclerotic lesions in apolipoprotein E deficient mice. *J Surg Res* 2011; 171: e231-236.
- [15] Dutta P, Courties G, Wei Y, Leuschner F, Gorbato R, Robbins CS, Iwamoto Y, Thompson B, Carlson AL, Heidt T, Majmudar MD, Lasitschka F, Etzrodt M, Waterman P, Waring MT, Chicoine AT, van der Laan AM, Niessen HW, Piek JJ, Rubin BB, Butany J, Stone JR, Katus HA, Murphy SA, Morrow DA, Sabatine MS, Vinegoni C, Moskowitz MA, Pittet MJ, Libby P, Lin CP, Swirski FK, Weissleder R and Nahrendorf M. Myocardial infarction accelerates atherosclerosis. *Nature* 2012; 487: 325-329.
- [16] Kim EJ, Kim S, Kang DO and Seo HS. Metabolic activity of the spleen and bone marrow in patients with acute myocardial infarction evaluated by ¹⁸F-fluorodeoxyglucose positron emission tomographic imaging. *Circ Cardiovasc Imaging* 2014; 7: 454-460.
- [17] Emami H, Singh P, MacNabb M, Vucic E, Laverder Z, Rudd JH, Fayad ZA, Lehrer-Graiwer J, Korsgren M, Figueroa AL, Fredrickson J, Rubin B, Hoffmann U, Truong QA, Min JK, Baruch A, Nasir K, Nahrendorf M and Tawakol A. Splenic metabolic activity predicts risk of future cardiovascular events: demonstration of a cardio-splenic axis in humans. *JACC Cardiovasc Imaging* 2015; 8: 121-130.
- [18] Joshi NV, Toor I, Shah AS, Carruthers K, Vesey AT, Alam SR, Sills A, Hoo TY, Melville AJ, Langlands SP, Jenkins WS, Uren NG, Mills NL, Fletcher AM, van Beek EJ, Rudd JH, Fox KA, Dweck MR and Newby DE. Systemic atherosclerotic inflammation following acute myocardial infarction: myocardial infarction begets myocardial infarction. *J Am Heart Assoc* 2015; 4: e001956.
- [19] Toutouzas K, Skoumas J, Koutagiari I, Benetos G, Pianou N, Georgakopoulos A, Galanakis S, Antonopoulos A, Drakopoulou M, Oikonomou EK, Kafouris P, Athanasiadis E, Metaxas M, Spyrou G, Pallantza Z, Galiatsatos N, Aggeli C, Antoniadis C, Keramida G, Peters AM, Anagnostopoulos CD and Tousoulis D. Vascular inflammation and metabolic activity in hematopoietic organs and liver in familial combined hyperlipidemia and heterozygous familial hypercholesterolemia. *J Clin Lipidol* 2018; 12: 33-43.
- [20] Keramida G, Dunford A, Siddique M, Cook GJ and Peters AM. Relationships of body habitus and SUV indices with signal-to-noise ratio of hepatic ¹⁸F-FDG PET. *Eur J Radiol* 2016; 85: 1012-1015.
- [21] Keramida G, Anagnostopoulos CD and Peters AM. The extent to which standardized uptake values reflect FDG phosphorylation in the liver and spleen as functions of time after injection of (18)F-fluorodeoxyglucose. *Eur J Nucl Med Mol Imaging Res* 2017; 7: 13.
- [22] Iozzo P, Jarvisalo MJ, Kiss J, Borra R, Naum GA, Viljanen A, Viljanen T, Gastaldelli A, Buzzigoli E, Guiducci L, Barsotti E, Savunen T, Knuuti J, Haaparanta-Solin M, Ferrannini E and Nuutila P. Quantification of liver glucose metabolism by positron emission tomography: validation study in pigs. *Gastroenterology* 2007; 132: 531-542.
- [23] Keiding S, Munk OL, Schiøtt KM and Hansen SB. Dynamic 2-[¹⁸F]fluoro-2-deoxy-D-glucose positron emission tomography of liver tumours without blood sampling. *Eur J Nucl Med* 2000; 27: 407-412.
- [24] de Geus-Oei LF, Visser EP, Krabbe PF, van Hoorn BA, Koenders EB, Willemsen AT, Pruim J, Corstens FH and Oyen WJ. Comparison of image-derived and arterial input functions for esti-

Hepato-splenic axis

- mating the rate of glucose metabolism in therapy-monitoring ^{18}F -FDG PET studies. *J Nucl Med* 2006; 47: 945-949.
- [25] Munk OL, Bass L, Roelsgaard K, Bender D, Hansen SB and Keiding S. Liver kinetics of glucose analogs measured in pigs by PET: importance of dual-input blood sampling. *J Nucl Med* 2001; 42: 795-801.
- [26] Iozzo P, Kirsti Hallsten K, Oikonen V, Virtanen KA, Kemppainen J, Solin O, Ferrannini E, Knuuti J and Nuutila P. Insulin-mediated hepatic glucose uptake is impaired in type 2 diabetes: evidence for a relationship with glycemic control. *J Clin Endocrinol Metab* 2003; 88: 2055-2060.
- [27] Iozzo P, Lautamaki R, Geisler F, Virtanen KA, Oikonen V, Haaparanta M, Yki-Jarvinen H, Ferrannini E, Knuuti J and Nuutila P. Non-esterified fatty acids impair insulin-mediated glucose uptake and disposition in the liver. *Diabetologia* 2004; 47: 1149-1156.
- [28] Tragardh M, Moller N and Sorensen M. Methodologic considerations for quantitative ^{18}F -FDG PET/CT studies of hepatic glucose metabolism in healthy subjects. *J Nucl Med* 2015; 56: 1366-1371.
- [29] Boyce CJ, Pickhardt PJ, Kim DH, Taylor AJ, Winter TC, Bruce RJ, Lindstrom MJ and Hinshaw JL. Hepatic steatosis (fatty liver disease) in asymptomatic adults identified by unenhanced low-dose CT. *Am J Roentgenol* 2010; 194: 623-628.
- [30] Keramida G, Potts J, Bush J, Verma S, Dizdarevic S and Peters AM. Accumulation of ^{18}F -fluorodeoxyglucose in the liver in hepatic steatosis. *Am J Roentgenol* 2014; 203: 643-648.
- [31] Choi Y, Hawkins RA, Huang SC, Brunken RC, Hoh CK, Messa C, Nitzsche EU, Phelps ME and Schelbert HR. Evaluation of the effect of glucose ingestion and kinetic model configurations of FDG in the normal liver. *J Nucl Med* 1994; 35: 818-823.
- [32] Iozzo P, Geisler F, Oikonen V, Mäki M, Takala T, Solin O, Ferrannini E, Knuuti J and Nuutila P. Insulin stimulates liver glucose uptake in humans: an ^{18}F -FDG PET study. *J Nucl Med* 2003; 44: 682-689.
- [33] Borra R, Lautamaki R, Parkkola R, Komu M, Sijens PE, Hällsten K, Bergman J, Iozzo P and Nuutila P. Inverse association between liver fat content and hepatic glucose uptake in patients with type 2 diabetes mellitus. *Metabolism* 2008; 57: 1445-1451.
- [34] Immonen H, Hannukainen JC, Iozzo P, Soinio M, Salminen P, Saunavaara V, Borra R, Parkkola R, Mari A, Lehtimäki T, Pham T, Laine J, Kärjä V, Pihlajamäki J, Nelimarkka L and Nuutila P. Effect of bariatric surgery on liver glucose metabolism in morbidly obese diabetic and non-diabetic patients. *J Hepatol* 2014; 60: 377-383.
- [35] Jones HA, Marino PS, Shakur BH and Morrell NW. In vivo assessment of lung inflammatory cell activity in patients with COPD and asthma. *Eur Respir J* 2003; 21: 567-573.
- [36] Subramanian DR, Jenkins L, Edgar R, Quraishi N, Stockley RA and Parr DG. Assessment of pulmonary neutrophilic inflammation in emphysema by quantitative positron emission tomography. *Am J Respir Crit Care Med* 2012; 186: 1125-1132.
- [37] Graham MM, Muzi M, Spence AM, O'Sullivan F, Lewellen TK, Link JM and Krohn KA. The FDG lumped constant in normal human brain. *J Nucl Med* 2002; 43: 1157-1166.
- [38] Peters AM, Klonizakis I, Lavender JP and Lewis SM. Use of ^{111}In -labeled platelets to measure spleen function. *Br J Haematol* 1980; 46: 587-593.
- [39] Akamatsu G, Ikari Y, Nishida H, Nishio T, Ohnishi A, Maebatake A, Sasaki M and Senda M. Influence of statistical fluctuation on reproducibility and accuracy of SUV_{max} and SUV_{peak} : a phantom study. *J Nucl Med Technol* 2015; 43: 222-226.
- [40] Kubota K, Watanabe H, Murata Y, Yukihiko M, Ito K, Morooka M, Minamimoto R, Hori A and Shibuya H. Effects of blood glucose level on FDG uptake by liver: a FDG-PET/CT study. *Nucl Med Biol* 2011; 38: 347-351.
- [41] Sugawara Y, Zasadny KR, Neuhoff AW and Wahl RL. Re-evaluation of the standardized uptake value for FDG: variations with body weight and methods for correction. *Radiology* 1999; 213: 521-525.
- [42] Bender D, Munk OL, Feng HQ and Keiding S. Metabolites of (18)F-FDG and 3-O-(11)C-methylglucose in pig liver. *J Nucl Med* 2001; 42: 1673-1678.
- [43] Hasselbalch SG, Knudsen GM, Capaldo B, Postiglione A and Paulson OB. Blood-brain barrier transport and brain metabolism of glucose during acute hyperglycemia in humans. *J Clin Endocrinol Metab* 2001; 86: 1986-1990.
- [44] Namba H, Nakagawa K, Iyo M, Fukushi K and Irie T. A simple method for measuring glucose utilization of insulin-sensitive tissues by using the brain as a reference. *Eur J Nucl Med* 1994; 21: 228-231.
- [45] Lindholm P, Minn H, Leskinen-Kallio S, Bergman J, Ulla Ruotsalainen U and Heikki Joensuu H. Influence of the blood glucose concentration on FDG uptake in cancer - a PET study. *J Nucl Med* 1993; 34: 1-6.